Inhibition of TLR2 signaling by small molecule inhibitors targeting a pocket within the TLR2 TIR domain

Pragnesh Mistry[a], Michelle H. W. Laird[a], Ryan S. Schwarz[a], Shannon Greene[b], Tristan Dyson[a], Greg A. Snyder[c], Tsan Sam Xiao[d], Jay Chauhan[b], Steven Fletcher[b], Vladimir Y. Toshchakov[a], Alexander D. MacKerell Jr.[b,1], and Stefanie N. Vogel[a,1]

[a]Department of Microbiology and Immunology and [c]Institute of Human Virology, School of Medicine, University of Maryland, Baltimore (UMB), Baltimore, MD 21201; [b]Department of Pharmaceutical Sciences, School of Pharmacy, University of Maryland, Baltimore, MD 21201; and [d]Department of Pathology, Case Western Reserve University, Cleveland, OH 44106

Edited by Shizuo Akira, Osaka University, Osaka, Japan, and approved March 17, 2015 (received for review November 25, 2014)

Toll-like receptor (TLR) signaling is initiated by dimerization of intracellular Toll/IL-1 receptor resistance (TIR) domains. For all TLRs except TLR3, recruitment of the adapter, myeloid differentiation primary response gene 88 (MyD88), to TLR TIR domains results in downstream signaling culminating in proinflammatory cytokine production. Therefore, blocking TLR TIR dimerization may ameliorate TLR2-mediated hyperinflammatory states. The BB loop within the TLR TIR domain is critical for mediating certain protein–protein interactions. Examination of the human TLR2 TIR domain crystal structure revealed a pocket adjacent to the highly conserved P681 and G682 BB loop residues. Using computer-aided drug design (CADD), we sought to identify a small molecule inhibitor(s) that would fit within this pocket and potentially disrupt TLR2 signaling. In silico screening identified 149 compounds and 20 US Food and Drug Administration-approved drugs based on their predicted ability to bind in the BB loop pocket. These compounds were screened in HEK293T-TLR2 transfectants for the ability to inhibit TLR2-mediated IL-8 mRNA. $C_{16}H_{15}NO_4$ (C29) was identified as a potential TLR2 inhibitor. C29, and its derivative, *ortho*-vanillin (*o*-vanillin), inhibited TLR2/1 and TLR2/6 signaling induced by synthetic and bacterial TLR2 agonists in human HEK-TLR2 and THP-1 cells, but only TLR2/1 signaling in murine macrophages. C29 failed to inhibit signaling induced by other TLR agonists and TNF-α. Mutagenesis of BB loop pocket residues revealed an indispensable role for TLR2/1, but not TLR2/6, signaling, suggesting divergent roles. Mice treated with *o*-vanillin exhibited reduced TLR2-induced inflammation. Our data provide proof of principle that targeting the BB loop pocket is an effective approach for identification of TLR2 signaling inhibitors.

small molecule inhibitor | BB loop | TLR2 pocket | CADD

Toll-like receptors (TLRs) are type I transmembrane receptors that detect conserved "pathogen-associated molecular patterns" from microbes, as well as host-derived "danger-associated molecular patterns" (1). TLR2 heterodimerizes with TLR6 or TLR1 to recognize diacyl lipopeptides or triacyl lipopeptides, respectively (2, 3), present in gram-positive and gram-negative bacteria (4–9).

Ligand engagement of TLR2/1 or TLR2/6 activates the myeloid differentiation primary response gene 88 (MyD88)-dependent pathway (i.e., nuclear translocation of NF-κB, activation of MAPKs), resulting in production of proinflammatory cytokines (10). Dysregulated TLR2 signaling has been implicated in numerous diseases (e.g., sepsis, atherosclerosis, tumor metastasis, ischemia/reperfusion injury) (11–14). Several inhibitors of TLR2 signaling have been developed (15–18), yet none is licensed for human use. A better understanding of the Toll/IL-1 receptor resistance (TIR) domain interactions involved in TLR2 signaling could lead to novel therapeutic agents.

Both TLRs and adapter proteins contain a cytoplasmic TIR domain that mediates homotypic and heterotypic interactions during TLR signaling (19). Two adapter proteins implicated in TLR2 signaling are MyD88 and TIRAP (Mal). A conserved Pro [e.g., P681 in human TLR2 (hTLR2), P712 in murine TLR4 (mTLR4), P674 in hTLR10, P804 in mTLR11] within the BB loop of almost all TIR domains is critical for signaling (20–27). More importantly, the BB loop P681H mutation in hTLR2 abolished recruitment of MyD88 and signaling (20, 26). Based on this evidence, the BB loop within the TLR2 TIR domain appears to be an ideal target for attenuation of TLR2 signaling.

Visual inspection of the crystal structure of the hTLR2 TIR domain (26) revealed a pocket formed by residues on the β-B strand and α-B helix that includes the highly conserved Pro and Gly residues of the BB loop. We hypothesized that targeting this pocket with a small molecule might inhibit interaction of TLR2 with MyD88, and thereby blunt TLR2 signaling. We identified $C_{16}H_{15}NO_4$ (C29) and its derivative, *ortho*-vanillin (*o*-vanillin), which inhibit mTLR2 and hTLR2 signaling initiated by synthetic and bacterial agonists without cytotoxicity. Interestingly, mutation of the BB loop pocket residues revealed a differential requirement for TLR2/1 vs. TLR2/6 signaling. Our data indicate that computer-aided drug design (CADD) is an effective approach for identifying small molecule inhibitors of TLR2 signaling and has the potential to identify inhibitors for other TLR signaling pathways.

Results

Screening of Potential TLR2 Inhibitors. Visual inspection of the crystal structure of the TLR2 TIR domain (Protein Data Bank ID

Significance

Excess Toll-like receptor 2 (TLR2) signaling has been implicated in numerous inflammatory diseases, yet there is no TLR2 inhibitor licensed for human use. Using computer-aided drug design (CADD), we identified a compound, $C_{16}H_{15}NO_4$ (C29), and a derivative, *ortho*-vanillin, that inhibit TLR2 signaling in vitro and in vivo. Our findings also revealed unexpected differences between TLR2/1 and TLR2/6 signaling in mice vs. humans. Importantly, our data provide proof of principle that the CADD-targeted BB loop pocket residues are critical for TLR2 signaling and may be targeted therapeutically.

Author contributions: P.M., M.H.W.L., R.S.S., G.A.S., T.S.X., S.F., V.Y.T., A.D.M., and S.N.V. designed research; P.M., M.H.W.L., R.S.S., S.G., T.D., G.A.S., J.C., and V.Y.T. performed research; A.D.M. and S.N.V. contributed new reagents/analytic tools; and P.M. and S.N.V. wrote the paper.

The authors declare no conflict of interest.

This article is a PNAS Direct Submission.

[1]To whom correspondence may be addressed. Email: svogel@som.umaryland.edu or amackere@rx.umaryland.edu

This article contains supporting information online at www.pnas.org/lookup/suppl/doi:10.1073/pnas.1422576112/-/DCSupplemental.

code 1FYW) revealed the BB loop pocket (Y647, C673, D678, F679, I680, K683, D687, N688, D691, and S692) adjacent to the conserved P681 and G682 residues of the BB loop (Fig. S1). Over 1 million commercially available small compounds, as well as US Food and Drug Administration (FDA)-approved drugs, were screened in silico for those compounds that could potentially fit into the pocket. CADD analysis identified ∼1,000 compounds based on predicted favorable interactions with the TLR2 BB loop pocket (*SI Materials and Methods*). Of these compounds, 149 chemically diverse small molecules and 20 FDA-approved drugs with physiochemical properties that should maximize bioavailability and ranked highest for their potential to fit into the TLR2 TIR pocket were screened for their ability to inhibit TLR2-mediated signaling.

Initially, 34 compounds (C1–C34) were tested in stably transfected HEK-hTLR2 cells for the ability to block N-Palmitoyl-S-[2,3-bis(palmitoyloxy)-(2*RS*)-propyl]-(*R*)-cysteinyl-(*S*)-seryl-(*S*)-lysyl-(*S*)-lysyl-(*S*)-lysyl-(*S*)-Lys (P3C)–induced and S-[2,3-bis(palmitoyloxy)-(2*RS*)-propyl]-(*R*)-cysteinyl-(*S*)-seryl-(*S*)-lysyl-(*S*)-lysyl-(*S*)-lysyl-(*S*)-Lys (P2C)–induced IL-8 mRNA via TLR2/1 and TLR2/6 signaling pathways, respectively. Four compounds (C10, C14, C29, and C32) consistently decreased P3C-induced IL-8 mRNA by ≥50% (Fig. S2*A*), and eight compounds (C14, C29, and C32 as seen in P3C-induced signaling, as well as C24, C25, C26, C30, and C33) decreased P2C-induced IL-8 mRNA by ≥50% (Fig. S2*B*). These results suggest that CADD is an effective first step for the identification of potential small molecule inhibitors of TLR2 signaling.

C29 Blunts hTLR2/1 and hTLR2/6 Signaling in HEK-TLR2 Stable Transfectants and THP-1 Cells. We next tested these potential TLR2 inhibitors to assess dose dependency and cytotoxicity. Compound C29 (Fig. 1*A*) blocked P3C- and P2C-induced IL-8 mRNA dose-dependently in HEK-TLR2 stable transfectants, although it had no effect on TNF-α–induced signaling or on cytotoxicity (Fig. 1*B* and Fig. S3). We next investigated the effect of C29 on TLR2 signaling in the human THP-1 macrophage-like cell line (28). C29 also inhibited P3C- and P2C-induced IL-1β gene expression significantly at both 1 h and 4 h following stimulation (Fig. 1*C*), as well as both P3C- and P2C-induced NF-κB–luciferase activity in transiently transfected HEK293T cells expressing hTLR2 and an NF-κB–sensitive luciferase reporter construct (Fig. S4). Thus, C29 inhibits both TLR2/1 and TLR2/6 signaling in human cell lines.

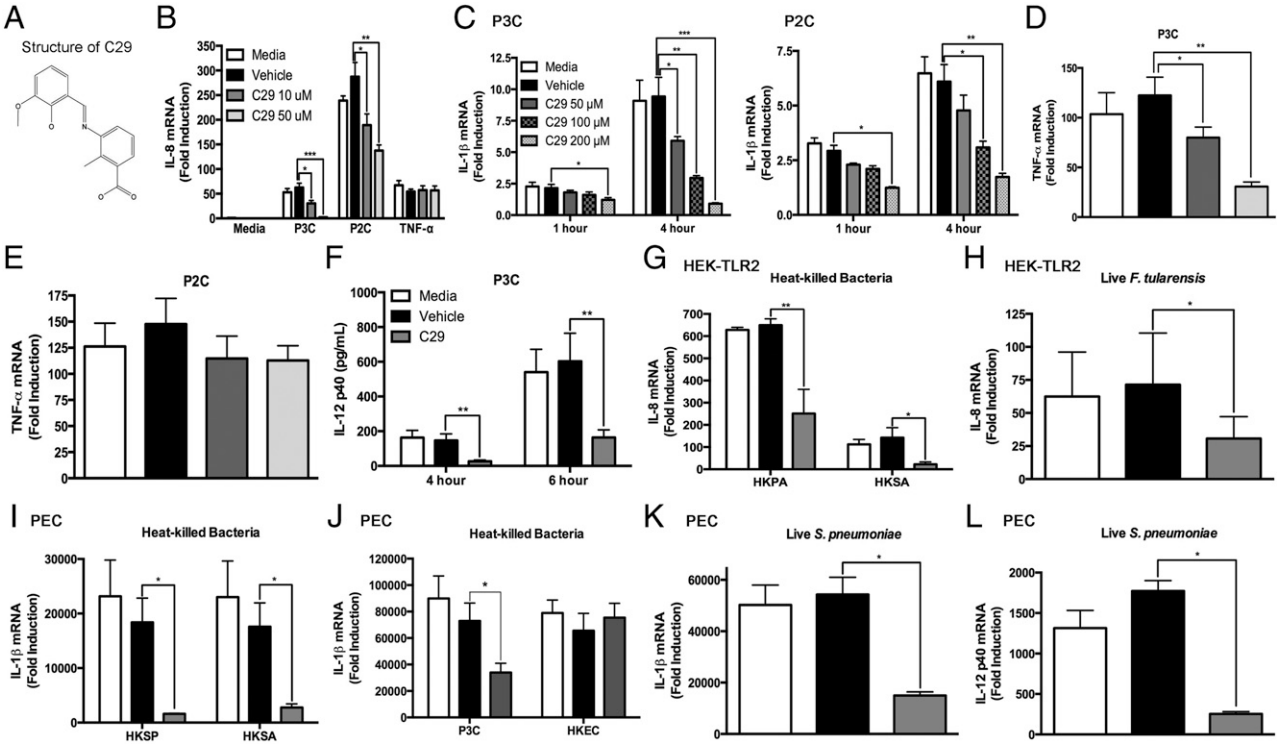

Fig. 1. Differential effect of C29 on gene expression in human cell lines and murine peritoneal macrophages. (*A*) Structure of C29. (*B*) Total RNA was extracted from HEK-TLR2 cells pretreated for 1 h with media, vehicle (65 μM NaOH), or C29 (10 μM or 50 μM) and then stimulated with P3C (200 ng/mL), P2C (200 ng/mL), or human TNF-α (300 ng/mL) for 1 h in the presence of media, vehicle, or C29. IL-8 mRNA was measured by qRT-PCR and was normalized to the expression of the GAPDH housekeeping gene. (*C*) THP-1 human macrophage-like cell line was plated in the presence of phorbol 12-myristate 13-acetate (PMA; 20 ng/mL) for 24 h and washed twice in media. Total RNA was extracted from cell cultures pretreated for 1 h with media, vehicle (260 μM NaOH), or C29 (50 μM, 100 μM, or 200 μM) and then stimulated with P3C (50 ng/mL; *Left*) or P2C (50 ng/mL; *Right*) for 1 or 4 h in the presence of media, vehicle, or C29. IL-1β mRNA was measured as described in *B*. (*D* and *E*) Total RNA was extracted from murine peritoneal macrophages that had been pretreated for 1 h with media (white bars), vehicle (130 μM NaOH, black bars), or C29 (25 μM, dark gray bars; 50 μM, light gray bars) and then stimulated with P3C (50 ng/mL) or P2C (100 ng/mL) for 1 h in the presence of media, vehicle, or C29. TNF-α mRNA was measured by qRT-PCR and normalized to the expression of the hypoxanthine-guanine phosphoribosyltransferase (HPRT) housekeeping gene. (*F*) Murine macrophages derived from peritoneal exudate cells (PEC) were pretreated for 1 h with media, vehicle, or C29 (50 μM) and then stimulated with P3C (50 ng/mL) for 4 or 6 h in the presence of media, vehicle, or C29. Culture supernatants were analyzed by ELISA for IL-12 p40 protein. HEK-TLR2 stable transfectants (*G* and *H*) and murine macrophages derived from PEC (*I*–*L*) are shown. Total RNA was extracted from cell cultures pretreated for 1 h with media, vehicle (65 μM NaOH), or C29 (50 μM) and then stimulated with heat-killed *P. aeruginosa* (HKPA) [multiplicity of infection (MOI) = 50], HKSA (MOI = 50), heat-killed *S. pneumoniae* (HKSP) (MOI = 50), P3C (50 ng/mL), heat-killed *E. coli* (HKEC) (MOI = 0.1), live *F. tularensis* live vaccine strain (LVS; MOI = 10) or live *S. pneumoniae* (MOI = 0.7) for 4 h in the presence of media, vehicle, or C29. RNA was analyzed by qRT-PCR for the expression of the indicated gene products. The qRT-PCR results shown in *B*–*E* and *G*–*L* are the mean ± SEM from two independent experiments, and the qRT-PCR result shown in *F* is the mean ± SEM from three independent experiments each carried out in duplicate (*$P \leq 0.05$; **$P \leq 0.01$; ***$P \leq 0.001$).

C29 Preferentially Inhibits TLR2/1 Signaling in Primary Murine Macrophages. Based on the high degree of amino acid sequence identity between hTLR2 and mTLR2 TIR domains (88.9%) and within the BB loop pocket (90%) (Fig. S1*B*), we hypothesized that C29 would also block TLR2 signaling in murine macrophages. Interestingly, C29 significantly reduced P3C-induced but not P2C-induced TNF-α mRNA and IL-12 p40 protein (Fig. 1 *D*–*F*) in contrast to the human cells, where C29 inhibited both TLR2/1 and TLR2/6 signaling pathways (Fig. 1 *B* and *C* and Fig. S4). To determine whether this difference was a species-specific or cell-specific effect, HEK293T cells were transfected with plasmids encoding either hTLR2 or mTLR2 and either TLR1 or TLR6, and the effect of C29 on TLR2/1 and TLR2/6 signaling was assessed using our NF-κB reporter assay. C29 significantly inhibited hTLR2/6-induced but not mTLR2/6-induced NF-κB–luciferase activity (Fig. S5). These results suggest that the difference in the ability of C29 to block hTLR2/6 signaling and not mTLR2/6 signaling is species-specific.

The specificity of C29 for TLR2/1 in murine cells was further assessed by testing additional TLR2 agonists, including *Staphylococcus aureus* lipoteichoic acid (LTA SA), a TLR2/1 agonist (8), and zymosan, shown previously to activate TLR2/6 (29) as well as other TLR agonists. C29 specifically blocked P3C-induced and LTA SA-induced IL-1β mRNA in murine macrophages (Fig. S6*A*). Like P2C (Fig. 1*E*), C29 did not inhibit zymosan-induced IL-1β mRNA in murine macrophages (Fig. S6*A*). Moreover, C29 had no significant inhibitory effect on the MyD88-independent pathway in murine macrophages when stimulated with agonists that induce IFN-β (Fig. S6*B*). C29 blocked zymosan- and LTA SA-induced IL-1β mRNA dose-dependently in human THP-1 cells (Fig. S6*C*). In summary, C29 blocks only TLR2/1-mediated cytokine mRNA and protein in primary murine macrophages.

C29 Blocks TLR2 Bacterial Agonist-Induced Proinflammatory Gene Expression in HEK-TLR2 Cells and Murine Macrophages. TLR2 dimerization with TLR1 or TLR6 allows for recognition of both gram-positive and certain gram-negative bacteria (e.g., *S. aureus*, *Streptococcus pneumoniae*, *Pseudomonas aeruginosa*, *Francisella tularensis*) (4, 6, 7, 9). C29 significantly inhibited heat-killed *P. aeruginosa*–induced and heat-killed *S. aureus* (HKSA)–induced IL-8 mRNA in HEK-TLR2 cells (Fig. 1*G*). C29 also significantly inhibited IL-8 mRNA in HEK-TLR2 cells stimulated by live *F. tularensis* (Fig. 1*H*), a TLR2/6 agonist (4, 5, 30). In primary murine macrophages derived from peritoneal exudate cells (PEC), C29 significantly blocked heat-killed *S. pneumoniae* (HKSP)–mediated and HKSA-mediated IL-1β mRNA (Fig. 1*I*). In contrast, IL-1β mRNA induced by heat-killed *Escherichia coli*, which signals predominately through TLR4, was not blocked by C29, in contrast to P3C-induced IL-1β mRNA (Fig. 1*J*). C29 also inhibited IL-1β and IL-12 p40 mRNA in murine macrophages stimulated with live *S. pneumoniae* (Fig. 1 *K* and *L*). Thus, C29 blocks cytokine gene expression induced by heat-killed or live bacterial TLR2 agonists in human HEK-TLR2 transfectants and in murine macrophages.

C29 Inhibits Ligand-Induced Interaction of TLR2 with MyD88 and Blocks MAPK and NF-κB Activation. Previous studies demonstrated that the P681H mutation within the BB loop of hTLR2 abolishes MyD88 recruitment, and thereby blunts signaling (20, 26). In THP-1 cells, C29 treatment diminished the interaction between endogenous TLR2 and MyD88 at 15 and 30 min poststimulation with P3C compared with vehicle control and achieved statistical significance at 30 min. Densitometry analysis of three independent experiments confirmed this finding (Fig. 2 *A* and *B*).

TLR2 recruitment of MyD88 activates NF-κB and MAPKs. Upon P3C stimulation, C29 blocked robust MAPK activation at 30 min and reduced NF-κB activation from 5 to 30 min (Fig. 2*C*). C29 prevented P3C-induced degradation of IκBα at 15 and 30 min (Fig. 2*C*).

TLR2 BB Loop Pocket Mutants Reveal Divergent Roles in TLR2/1 and TLR2/6 Signaling. Alanine scanning mutagenesis of all 10 BB loop pocket residues, as well as three additional mutations (Y641A, P681H, and Q747A) was performed, and their effect on TLR2/1 and TLR2/6 signaling in the absence or presence of C29 was examined using our NF-κB reporter assay. Y641A and P681H were shown previously to play a role in TLR2–MyD88 interaction (20, 26), and Gautam et al. (31) reported that Q747 was not important for TLR2 signaling, and therefore served as a control mutation. All 10 BB loop pocket mutants, including Y647A and P681H, were critical for TLR2/1 signaling (Fig. 3*A*). Interestingly, the C673A, I680A, K683A, and S692A BB loop pocket mutants retained the ability to signal through TLR2/6, suggesting divergent roles for these amino acids in TLR2/1 and TLR2/6 responsiveness (Fig. 3*B*). Western blot analysis revealed that total protein expression of each TLR2 mutant was comparable to WT TLR2 (Fig. 3*C*). Importantly, TLR2 signaling-deficient mutants had levels of membrane protein expression similar to WT TLR2 (Fig. 3*D*). These results suggest that hTLR2 BB loop pocket residues are critical for TLR2/1 signaling, but only some are necessary for TLR2/6 signaling.

C29 Derivative, *O*-Vanillin, Reproduces the TLR2 Inhibitory Activity of C29. To preclude cytotoxicity from DMSO, we dissolved C29 in 65 μM NaOH in H_2O. The structure of C29 (Fig. 1*A*) suggested

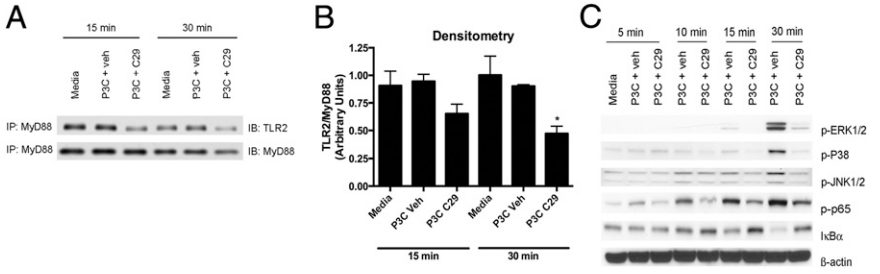

Fig. 2. C29 inhibits ligand-induced interaction of TLR2 with MyD88 and blocks MAPK and NF-κB activation. (*A*) THP-1 cells were cultured in the presence of PMA (20 ng/mL) for 24 h and washed twice in media. THP-1 human monocytes were pretreated with media, vehicle (195 μM NaOH), or C29 (150 μM) for 1 h and treated with P3C (50 ng/mL) in the presence of media, vehicle, or C29 for 15 or 30 min. Coimmunoprecipitation (IP) was carried out using anti-MyD88 Ab and Western blot analysis [immunoblotting (IB)] using whole-cell lysates. (*B*) Densitometry analysis (mean ± SEM) of three independent experiments as shown in *A*. Veh, vehicle. (*C*) Murine peritoneal macrophages were pretreated for 1 h with media, vehicle (65 μM NaOH), or C29 (50 μM) and treated with P3C (50 ng/mL) for 5–30 min in the presence of media, vehicle, or C29. IB was performed using whole-cell lysates and Abs directed against the signaling intermediates indicated. β-Actin was probed as a loading protein. *A* is representative of three independent experiments, and *B* is the mean ± SEM from three independent experiments (*$P \leq 0.05$). *C* is representative of two independent experiments.

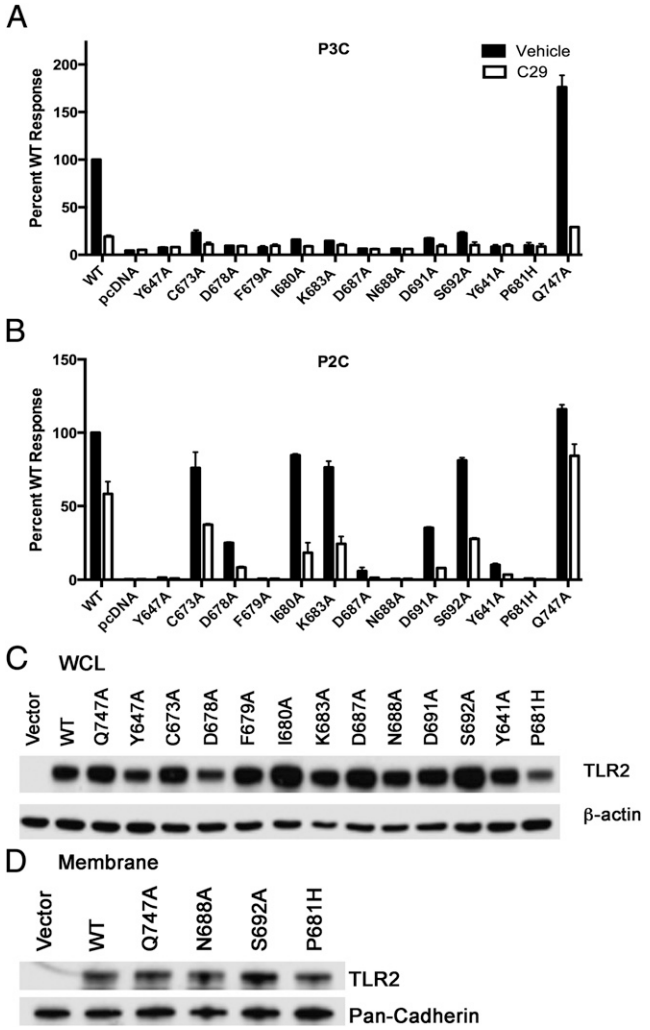

Fig. 3. Pocket residues serve divergent roles in TLR2/1 and TLR2/6 responsiveness. (*A* and *B*) HEK293T cells were transiently transfected with reporter constructs for endothelial leukocyte adhesion molecule (ELAM)-luciferase; *Renilla*-luciferase; and pcDNA3.1, WT pcDNA3-YFP-hTLR2, or mutant TLR2 constructs in the same vector. Cells were pretreated for 1 h with media, vehicle (65 μM NaOH), or C29 (50 μM) and treated with P3C or P2C (50 ng/mL) for 5 h in the presence of media, vehicle, or C29. Lysates were prepared, and the dual-luciferase assay was performed. (*C* and *D*) HEK293T cells were transiently transfected with pcDNA3.1, WT pcDNA3-YFP-hTLR2, or mutant TLR2 constructs in the same vector. Western blot analysis was performed using whole-cell lysates (WCL) (*C*) or membrane extracts (*D*) to ensure comparable expression of each TLR2 mutant. Pan-Cadherin was probed as a loading protein for membrane extracts. *A* and *B* represent the mean ± SEM from two independent experiments, each carried out in duplicate, and *C* and *D* are representative of two independent experiments.

that the imine linkage would likely be highly susceptible to nucleophilic cleavage into two species consisting of 3-amino-2-methylbenzoic acid (C29R) and *o*-vanillin (C29L) (Fig. S7*A*). TLC confirmed that C29 is cleaved into these two species when dissolved in 65 μM NaOH, but not when dissolved in an organic solvent (Fig. S7*B*). The two cleavage products, C29L and C29R, were tested to determine if either would reproduce the TLR2 inhibitory activity of C29. C29L, but not C29R, dose-dependently inhibited TLR2/1-induced TNF-α gene expression in murine macrophages, although it had no effect on TLR2/6 or TLR4 signaling pathways (Fig. S7 *C* and *D*).

We next sought to determine if C29L also blocks hTLR2 signaling with similar potency and specificity. Using the NF-κB reporter assay in HEK293T cells, we quantified the IC_{50} of C29 and C29L for hTLR2/1 and hTLR2/6 signaling. C29L blocked hTLR2/1 (IC_{50} = 24. 2 μM) and hTLR2/6 signaling (IC_{50} = 37.2 μM) comparable to C29 (IC_{50} = 19.7 μM and 37.6 μM, respectively) (Fig. S8).

Modeling of the BB loop pocket and C29L revealed that C29L fits within the BB loop pocket (Fig. S9). Together, these hypothetical predictions suggest that C29L is comparable to C29 for inhibiting hTLR2 and mTLR2 signaling.

C29L Inhibits TLR2/1-Induced Inflammation in Vivo. One of the advantages of using C29L in vivo is that C29L is more soluble in water than C29. We next examined if C29L could inhibit TLR2/1-induced proinflammatory cytokines in vivo. Mice treated twice with C29L before administration of P3C significantly blocked IL-12 p40 and TNF-α liver cytokine mRNA and serum protein (Fig. 4). Importantly, C29L had a significant inhibitory effect at the later time point for IL-12 p40. Collectively, C29L blocks TLR2/1 signaling both in vitro and in vivo.

Discussion

TLR activation involves multifaceted interactions of cytoplasmic TIR domain-containing proteins. The BB loop has been established as central for mediating TIR domain interactions. Mutagenesis of TLR2 BB loop residues and cell-permeating decoy peptides that target this region has revealed the functional importance of the BB loop in mediating downstream signaling (20, 24–26, 32). In this study, we combined in silico screening targeting a predicted TLR2 BB loop pocket with biological screening in various cell types to identify C29 and a derivative, *o*-vanillin, as inhibitors of both mTLR2 and hTLR2 signaling in response to synthetic or bacterial agonists.

In hTLR2 signaling, C29 and *o*-vanillin blocked both the TLR2/1 and TLR2/6 pathways (Fig. 1 and Figs. S4, S5, S6*C*, and S8), although the percentage of inhibition in HEK-TLR2 cells was consistently greater when TLR2/1 was stimulated (Figs. 1*B* and 3 and Figs. S4, S5, S6*C*, and S8). In murine cells, C29 and *o*-vanillin block only the TLR2/1 pathway significantly (Fig. 1

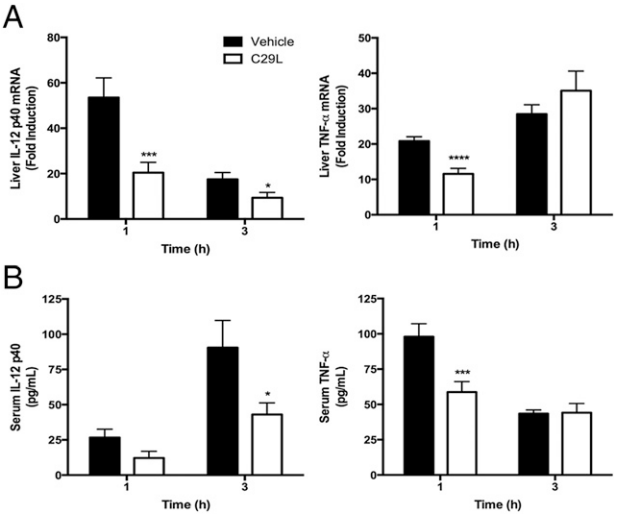

Fig. 4. C29L inhibits TLR2/1-induced inflammation in vivo. C57BL/6J mice were pretreated i.p. with vehicle (water) or C29L (1.314 mM/g) for 1 h. Mice received a second pretreatment administered i.p. with vehicle (water) or C29L (1.314 mM/g), were challenged subsequently i.p. with PBS or P3C (100 μg), and were killed 1 h or 3 h later. Liver RNA was analyzed by qRT-PCR (*A*), and serum concentrations were analyzed using Multiplex beads (*B*) (*$P \leq 0.05$; ***$P \leq 0.001$; ****$P \leq 0.0001$). In *A* and *B*, $n = 6$ (the combined data from two separate experiments) for each treatment group.

and Figs. S6 and S7). This finding was confirmed using LTA SA, a TLR2/1 ligand (33, 34), whereas C29 failed to block proinflammatory gene expression induced by zymosan (Fig. S6), a TLR2/6 agonist (29). These results support a previous study showing that cell-permeating decoy peptides derived from the BB loop of the TLR2 TIR domain inhibited ERK activation induced by P3C, but not P2C, in murine macrophages (32).

A possible explanation for this difference in C29-mediated inhibition for hTLR2 vs. mTLR2 signaling could be that the BB loops of mTLR2 and hTLR2 play distinct roles in heterodimer formation and MyD88 recruitment. The highly flexible BB loop is central to many molecular interactions involving TIR domains and adopts different conformations as observed in functional and structural studies of TLR1, TLR2, TLR10, and, recently, TLR6 (26, 31, 35–37). Homodimeric molecular interactions observed in structural studies of hTLR1, hTLR2, and hTLR10 are largely mediated by residues found on the BB loop, DD loop, and α-C helix (26, 31, 36, 37) (Fig. S10). In contrast, homodimeric molecular interactions observed in the recent crystal structure of the TLR6 TIR domain (35) are reported not to include BB loop interactions, but rather involve the CD loop, DD loop, and α-C helix residues (Fig. S10). This difference may explain why we observed a proportionally greater inhibitory effect of C29 or *o*-vanillin on hTLR2/1 signaling compared with hTLR2/6 signaling and a minimal effect on mTLR2/6 signaling. Analysis of the BB loop pocket mutants further supports that BB loop pocket residues are highly critical for TLR2/1 signaling, whereas only C673, I680, K683, and S692 were dispensable for TLR2/6 signaling (Fig. 3 *A* and *B*).

Based on our functional mutagenesis data, C29 and *o*-vanillin may function by specifically targeting the BB loop pocket of the TLR2 TIR domain, altering its function and/or position. Jiang et al. (38) described a murine mutation in MyD88 (I179N), called Pococurante (Poc), that exhibited deficient TLR2/1 signaling but normal TLR2/6 signaling, suggesting that TLR2 interacts with MyD88 in different ways. Using molecular dynamics simulations, Snyder et al. (39) demonstrated that in WT MyD88, the BB loop is stabilized, whereas the Poc mutation potentiates its flexibility. A mobile BB loop could potentially result in a greater entropic cost to obtain stable TIR–TIR interactions and lead to deficient signaling (39). Differences observed in C29-mediated and *o*-vanillin–mediated inhibition of hTLR2 and mTLR2 signaling and mutagenesis studies of BB loop pocket residues may reflect differential use of the BB loop involving TIR1, TIR2, TIR6, and MyD88 molecular interactions. Future structural studies involving bona fide heterodimers of the TLR1/2 and TLR2/6 TIR domain would be very helpful in understanding the differences in TLR2/1 and TLR2/6 signaling.

Finally, we sought to determine if *o*-vanillin would inhibit TLR2-mediated induction of proinflammatory cytokines in vivo. *O*-vanillin is more soluble in water than C29, and therefore was used in our animal studies. Mice pretreated twice with *o*-vanillin and challenged with P3C showed reduced IL-12 p40 and TNF-α liver mRNA and serum protein compared with mice pretreated with vehicle control (H_2O) (Fig. 4). One of the limitations of using *o*-vanillin in vivo is its poor bioavailability, as has been reported previously for its isomer, vanillin (40). Due to this challenge, we administered a high dose twice to achieve an appreciable inhibitory effect in vivo. Despite this drawback, we were still able to measure a significant inhibitory effect for IL-12 p40 at the later time point (Fig. 4). Future studies will focus on chemical modification of *o*-vanillin to increase its inhibitory efficacy and/or deliver it on a carrier to reduce rapid clearance. A polymeric prodrug of vanillin was found to reduce acetaminophen-induced liver injury in mice (41). With the increasing knowledge we have of the crystal structures of the different TLR family members and sites of protein–protein interactions, CADD could potentially lead to targeted therapeutics against other TLR family members.

Materials and Methods

CADD in Silico Screening. CADD screening was performed as described previously (42–44) to identify small molecule inhibitors of TLR2 signaling. Briefly, CADD analysis required the following steps: (*i*) visual identification of a putative "pocket" in the 3D structure of the TLR2 TIR domain (Fig. S1*A*); (*ii*) primary docking using the DOCK algorithm (UCSF Computer Graphics Laboratory) (45) of more than 1 million low-molecular-weight, commercially available, and FDA-approved compounds; (*iii*) more rigorous secondary docking of various conformations of TLR2 obtained from molecular dynamics simulation of the protein using CHARMM (46); and (*iv*) screening the top 149 and 20 FDA-approved drugs for the ability to block TLR2 signaling in stably or transiently transfected HEK-TLR2 cells, THP-1 cells, or murine macrophages, as described in *SI Materials and Methods*.

Quantitative Real-Time PCR. Cytokine gene expression was measured by quantitative real-time (qRT) PCR with transcript-specific primers using SYBR Green in the ABI Prism 7900 Fast Real-Time PCR System (Applied Biosystems) as described (4).

Transient Transfection and NF-κB Reporter Assay. HEK293T cells were cultured and plated overnight in 12-well tissue culture plates (2×10^5 cells per well). Transfection mixtures consisted of pcDNA3-YFP-hTLR2 or pcDNA3.1 control vector (1 μg per well each), pELAM (NF-κB)-luciferase (0.2 μg per well), and pRL-TK-*Renilla* luciferase (0.05 μg per well). Transfection was carried out using Superfect transfection reagent (Qiagen), and cells were allowed to recover for 48 h and treated for 5 h with medium or stimuli in the presence/absence of C29. Cells were lysed in a passive lysis buffer (Promega), and firefly luciferase and *Renilla* luciferase activities were measured using the Dual-Luciferase Reporter Assay System (Promega). *Renilla* luciferase was used for normalization, and all values were further standardized to medium-treated pcDNA3-YFP-hTLR2 transfectants to determine relative luciferase units (47).

Cytokine Protein Measurements. Cytokine levels in culture supernatants were analyzed by Multiplex beads (Milipore) in the Cytokine Core Laboratory (UMB).

In Vivo Studies of TLR2 Inhibitor. All animal studies were carried out with institutional approval by the University of Maryland, Baltimore (UMB) Institutional Animal Care and Use Committee. Female C57BL/6J mice (6–8 wk old) were purchased from The Jackson Laboratory and (n = 3 mice per group) received PBS, H_2O, or C29L (in H_2O) administered i.p. (1.314 mM/g). After 1 h, mice received a second injection of PBS, H_2O, or C29L administered i.p. (1.314 mM/g) and were subsequently challenged i.p. with PBS or P3C (100 μg) for 1 or 3 h. Mice were bled, and sera were prepared. Livers were also extracted for qRT-PCR analysis.

Statistical Analysis. One-way ANOVA with Tukey's multiple comparisons post hoc test was used to determine statistical significance (P values < 0.05) using GraphPad Prism 6.0 (GraphPad Software, Inc.). Values are represented as the mean ± SEM.

More detailed descriptions of all methods can be found in *SI Materials and Methods*.

ACKNOWLEDGMENTS. We thank Drs. Swamy Polumuri, Rajesh Rajaiah, Katharina Richard, Darren Perkins, and Wenji Piao for providing help throughout the study. This work was supported by NIH Grants AI018797 and T32ES007263 and the University of Maryland Computer-Aided Drug Design Center.

1. Medzhitov R (2001) Toll-like receptors and innate immunity. *Nat Rev Immunol* 1(2):135–145.
2. Takeuchi O, et al. (2001) Discrimination of bacterial lipoproteins by Toll-like receptor 6. *Int Immunol* 13(7):933–940.
3. Takeuchi O, et al. (2002) Cutting edge: Role of Toll-like receptor 1 in mediating immune response to microbial lipoproteins. *J Immunol* 169(1):10–14.
4. Cole LE, et al. (2006) Immunologic consequences of Francisella tularensis live vaccine strain infection: Role of the innate immune response in infection and immunity. *J Immunol* 176(11):6888–6899.
5. Cole LE, et al. (2007) Toll-like receptor 2-mediated signaling requirements for Francisella tularensis live vaccine strain infection of murine macrophages. *Infect Immun* 75(8):4127–4137.
6. Medina EA, Morris IR, Berton MT (2010) Phosphatidylinositol 3-kinase activation attenuates the TLR2-mediated macrophage proinflammatory cytokine response to Francisella tularensis live vaccine strain. *J Immunol* 185(12):7562–7572.
7. Raoust E, et al. (2009) Pseudomonas aeruginosa LPS or flagellin are sufficient to activate TLR-dependent signaling in murine alveolar macrophages and airway epithelial cells. *PLoS ONE* 4(10):e7259.

8. Schröder NW, et al. (2003) Lipoteichoic acid (LTA) of Streptococcus pneumoniae and Staphylococcus aureus activates immune cells via Toll-like receptor (TLR)-2, lipopolysaccharide-binding protein (LBP), and CD14, whereas TLR-4 and MD-2 are not involved. *J Biol Chem* 278(18):15587–15594.
9. Yoshimura A, et al. (1999) Cutting edge: Recognition of Gram-positive bacterial cell wall components by the innate immune system occurs via Toll-like receptor 2. *J Immunol* 163(1):1–5.
10. Kumar H, Kawai T, Akira S (2011) Pathogen recognition by the innate immune system. *Int Rev Immunol* 30(1):16–34.
11. Castoldi A, et al. (2012) TLR2, TLR4 and the MYD88 signaling pathway are crucial for neutrophil migration in acute kidney injury induced by sepsis. *PLoS ONE* 7(5):e37584.
12. Leemans JC, et al. (2005) Renal-associated TLR2 mediates ischemia/reperfusion injury in the kidney. *J Clin Invest* 115(10):2894–2903.
13. Mullick AE, Tobias PS, Curtiss LK (2005) Modulation of atherosclerosis in mice by Toll-like receptor 2. *J Clin Invest* 115(11):3149–3156.
14. Yang HZ, et al. (2009) Blocking TLR2 activity attenuates pulmonary metastases of tumor. *PLoS ONE* 4(8):e6520.
15. Arslan F, et al. (2012) Treatment with OPN-305, a humanized anti-Toll-Like receptor-2 antibody, reduces myocardial ischemia/reperfusion injury in pigs. *Circ Cardiovasc Interv* 5(2):279–287.
16. Cheng K, Wang X, Zhang S, Yin H (2012) Discovery of small-molecule inhibitors of the TLR1/TLR2 complex. *Angew Chem Int Ed Engl* 51(49):12246–12249.
17. Meng G, et al. (2004) Antagonistic antibody prevents toll-like receptor 2-driven lethal shock-like syndromes. *J Clin Invest* 113(10):1473–1481.
18. Murgueitio MS, Henneke P, Glossmann H, Santos-Sierra S, Wolber G (2014) Prospective virtual screening in a sparse data scenario: Design of small-molecule TLR2 antagonists. *ChemMedChem* 9(4):813–822.
19. Akira S, Uematsu S, Takeuchi O (2006) Pathogen recognition and innate immunity. *Cell* 124(4):783–801.
20. Brown V, Brown RA, Ozinsky A, Hesselberth JR, Fields S (2006) Binding specificity of Toll-like receptor cytoplasmic domains. *Eur J Immunol* 36(3):742–753.
21. Hasan U, et al. (2005) Human TLR10 is a functional receptor, expressed by B cells and plasmacytoid dendritic cells, which activates gene transcription through MyD88. *J Immunol* 174(5):2942–2950.
22. Poltorak A, et al. (1998) Defective LPS signaling in C3H/HeJ and C57BL/10ScCr mice: Mutations in Tlr4 gene. *Science* 282(5396):2085–2088.
23. Qureshi ST, et al. (1999) Endotoxin-tolerant mice have mutations in Toll-like receptor 4 (Tlr4). *J Exp Med* 189(4):615–625.
24. Underhill DM, et al. (1999) The Toll-like receptor 2 is recruited to macrophage phagosomes and discriminates between pathogens. *Nature* 401(6755):811–815.
25. Underhill DM, Ozinsky A, Smith KD, Aderem A (1999) Toll-like receptor-2 mediates mycobacteria-induced proinflammatory signaling in macrophages. *Proc Natl Acad Sci USA* 96(25):14459–14463.
26. Xu Y, et al. (2000) Structural basis for signal transduction by the Toll/interleukin-1 receptor domains. *Nature* 408(6808):111–115.
27. Zhang D, et al. (2004) A toll-like receptor that prevents infection by uropathogenic bacteria. *Science* 303(5663):1522–1526.
28. Tsuchiya S, et al. (1980) Establishment and characterization of a human acute monocytic leukemia cell line (THP-1). *Int J Cancer* 26(2):171–176.
29. Ozinsky A, et al. (2000) The repertoire for pattern recognition of pathogens by the innate immune system is defined by cooperation between toll-like receptors. *Proc Natl Acad Sci USA* 97(25):13766–13771.
30. Katz J, Zhang P, Martin M, Vogel SN, Michalek SM (2006) Toll-like receptor 2 is required for inflammatory responses to Francisella tularensis LVS. *Infect Immun* 74(5):2809–2816.
31. Gautam JK, Ashish, Comeau LD, Krueger JK, Smith MF, Jr (2006) Structural and functional evidence for the role of the TLR2 DD loop in TLR1/TLR2 heterodimerization and signaling. *J Biol Chem* 281(40):30132–30142.
32. Toshchakov VY, Fenton MJ, Vogel SN (2007) Cutting Edge: Differential inhibition of TLR signaling pathways by cell-permeable peptides representing BB loops of TLRs. *J Immunol* 178(5):2655–2660.
33. Han SH, Kim JH, Martin M, Michalek SM, Nahm MH (2003) Pneumococcal lipoteichoic acid (LTA) is not as potent as staphylococcal LTA in stimulating Toll-like receptor 2. *Infect Immun* 71(10):5541–5548.
34. Travassos LH, et al. (2004) Toll-like receptor 2-dependent bacterial sensing does not occur via peptidoglycan recognition. *EMBO Rep* 5(10):1000–1006.
35. Jang TH, Park HH (2014) Crystal structure of TIR domain of TLR6 reveals novel dimeric interface of TIR-TIR interaction for toll-like receptor signaling pathway. *J Mol Biol* 426(19):3305–3313.
36. Nyman T, et al. (2008) The crystal structure of the human toll-like receptor 10 cytoplasmic domain reveals a putative signaling dimer. *J Biol Chem* 283(18):11861–11865.
37. Tao X, Xu Y, Zheng Y, Beg AA, Tong L (2002) An extensively associated dimer in the structure of the C713S mutant of the TIR domain of human TLR2. *Biochem Biophys Res Commun* 299(2):216–221.
38. Jiang Z, et al. (2006) Details of Toll-like receptor:adapter interaction revealed by germ-line mutagenesis. *Proc Natl Acad Sci USA* 103(29):10961–10966.
39. Snyder GA, et al. (2013) Molecular mechanisms for the subversion of MyD88 signaling by TcpC from virulent uropathogenic Escherichia coli. *Proc Natl Acad Sci USA* 110(17):6985–6990.
40. Beaudry F, Ross A, Lema PP, Vachon P (2010) Pharmacokinetics of vanillin and its effects on mechanical hypersensitivity in a rat model of neuropathic pain. *Phytother Res* 24(4):525–530.
41. Kwon J, et al. (2013) Inflammation-responsive antioxidant nanoparticles based on a polymeric prodrug of vanillin. *Biomacromolecules* 14(5):1618–1626.
42. Hancock CN, et al. (2005) Identification of novel extracellular signal-regulated kinase docking domain inhibitors. *J Med Chem* 48(14):4586–4595.
43. Li T, et al. (2014) Novel LRRK2 GTP-binding inhibitors reduced degeneration in Parkinson's disease cell and mouse models. *Hum Mol Genet* 23(23):6212–6222.
44. Zhong S, et al. (2008) Identification and validation of human DNA ligase inhibitors using computer-aided drug design. *J Med Chem* 51(15):4553–4562.
45. Kuntz ID, Blaney JM, Oatley SJ, Langridge R, Ferrin TE (1982) A geometric approach to macromolecule-ligand interactions. *J Mol Biol* 161(2):269–288.
46. Brooks BR, et al. (2009) CHARMM: The biomolecular simulation program. *J Comput Chem* 30(10):1545–1614.
47. Singh IS, et al. (2008) Heat shock co-activates interleukin-8 transcription. *Am J Respir Cell Mol Biol* 39(2):235–242.